Available online at www.sciencedirect.com
ScienceDirect
Applied Catalysis B: Environmental 72 (2007) 373–381
APPLIED CATALYSIS B: ENVIRONMENTAL
www.elsevier.com/locate/apcatb

Mineralization of clofibric acid by electrochemical advanced oxidation processes using a boron-doped diamond anode and Fe^{2+} and UVA light as catalysts

Ignasi Sirés, Francesc Centellas, José Antonio Garrido, Rosa María Rodríguez, Conchita Arias, Pere-Lluís Cabot, Enric Brillas *

Laboratori d'Electroquímica dels Materials i del Medi Ambient, Departament de Química Física, Facultat de Química, Universitat de Barcelona, Martí I Franquès 1-11, 08028 Barcelona, Spain

Received 19 October 2006; received in revised form 28 November 2006; accepted 2 December 2006
Available online 20 December 2006

Abstract

This work shows that aqueous solutions of clofibric acid (2-(4-chlorophenoxy)-2-methylpropionic acid), the bioactive metabolite of various lipid-regulating drugs, up to saturation at pH 3.0 are efficiently and completely degraded by electrochemical advanced oxidation processes such as electro-Fenton and photoelectro-Fenton with Fe^{2+} and UVA light as catalysts using an undivided electrolytic cell with a boron-doped diamond (BDD) anode and an O_2-diffusion cathode able to electrogenerate H_2O_2. This is feasible in these environmentally friendly methods by the production of oxidant hydroxyl radical at the BDD surface from water oxidation and in the medium from Fenton's reaction between Fe^{2+} and electrogenerated H_2O_2. The degradation process is accelerated in photoelectro-Fenton by additional photolysis of Fe^{3+} complexes under UVA irradiation. Comparative treatments by anodic oxidation with electrogenerated H_2O_2, but without Fe^{2+}, yield much slower decontamination. Chloride ion is released and totally oxidized to chlorine at the BDD surface in all treatments. The decay kinetics of clofibric acid always follows a pseudo-first-order reaction. 4-Chlorophenol, 4-chlorocatechol, hydroquinone, *p*-benzoquinone and 2-hydroxyisobutyric, tartronic, maleic, fumaric, formic and oxalic acids, are detected as intermediates. The ultimate product is oxalic acid, which is slowly but progressively oxidized on BDD in anodic oxidation. In electro-Fenton this acid forms Fe^{3+}–oxalato complexes that can also be totally destroyed at the BDD anode, whereas in photoelectro-Fenton the mineralization rate of these complexes is enhanced by its parallel photodecarboxylation with UVA light.

Keywords: Boron-doped diamond anode; Catalysis; Electro-Fenton; Photoelectro-Fenton; Drug mineralization

1. Introduction

The detection of a large variety of pharmaceutical drugs and metabolites including analgesics, anti-inflammatories, anti-microbials, antiepileptics, beta-blockers, estrogens and lipid regulators as emerging pollutants in waters at concentrations from nanograms to micrograms per litre has been recently documented [1–10]. The main sources of this contamination include emission from production sites, direct disposal of overplus drugs in households, excretion after drug administration to humans and animals, treatments throughout the water in fish and other animal farms and inadequate treatment of manufacturing waste [8]. To avoid the potential adverse health effects of these pollutants on living beings, research efforts are underway to develop efficient oxidation techniques for achieving their total mineralization, i.e. their complete conversion into CO_2.

Clofibric acid (2-(4-chlorophenoxy)-2-methylpropionic acid) is the bioactive metabolite of drugs such as clofibrate, etofibrate and etofyllineclofibrate, widely used as blood lipid regulators because they decrease the plasmatic content of cholesterol and triglycerides [9]. This compound has an estimated environmental persistence of 21 days [10] and has been found up to 10 $\mu g\ l^{-1}$ in sewage treatment plant effluents, rivers, lakes, North Sea, ground waters and drinking waters [1,2,6]. However, it is poorly degraded by ozonation [5,11], H_2O_2/UV [11], sunlight and UV photolysis [7] and TiO_2/UV [12], as well as after application of biological and physico-chemical methods in sewage treatment

* Corresponding author. Tel.: +34 93 4021223; fax: +34 93 4021231.
E-mail address: brillas@ub.edu (E. Brillas).

0926-3373/$ – see front matter © 2006 Elsevier B.V. All rights reserved.
doi:10.1016/j.apcatb.2006.12.002

plants [9]. In previous work [13] we have explored the electrochemical degradation of clofibric acid solutions in the pH range 2.0–12.0 by means of the classical method of anodic oxidation with a cell containing either a Pt or boron-doped diamond (BDD) anode and a stainless steel cathode. Under these conditions, the metabolite solutions were poorly decontaminated with a Pt anode, whereas the alternative use of BDD yielded their complete mineralization, but with very low degradation rate and current efficiency. The greater oxidizing power of BDD compared to Pt is ascribed to its higher O_2-overpotential, which allows the generation of more amount of the strong oxidant hydroxyl radical (BDD($^\bullet$OH)) adsorbed on its surface from water oxidation [14–18]:

$$BDD(H_2O) \rightarrow BDD(^\bullet OH) + H^+ + e^- \quad (1)$$

Under these conditions, other weaker oxidants such as peroxodisulfate ion, H_2O_2 and O_3 at the BDD anode are also produced [18]. Anodic oxidation with a BDD anode seems a viable technique to mineralize clofibric acid, but its very low oxidation power prevents its possible application to the treatment of industrial wastewaters containing this compound. This makes necessary the search of other potent technologies with higher ability to remove this pollutant from waters.

Recently, powerful indirect electrooxidation methods such as electro-Fenton and photoelectro-Fenton are being developed for water remediation [19–31]. These electrochemical advanced oxidation processes (AEOPs) are environmentally friendly technologies based on the continuous supply of H_2O_2 to an acidic contaminated solution from the two-electron reduction of injected O_2:

$$O_2 + 2H^+ + 2e^- \rightarrow H_2O_2 \quad (2)$$

Reticulated vitreous carbon [19,20], carbon-felt [21,22,24,27,30], activated carbon fibre [28] and O_2-diffusion [23,25,26,29,31] cathodes are usually employed to reduce efficiently O_2 from reaction (2). In the electro-Fenton process the oxidizing ability of electrogenerated H_2O_2 is strongly enhanced by adding to the solution a small quantity of Fe^{2+} to produce hydroxyl radical ($^\bullet$OH) and Fe^{3+} from the classical Fenton's reaction [32]:

$$Fe^{2+} + H_2O_2 \rightarrow Fe^{3+} + {}^\bullet OH + OH^- \quad (3)$$

An advantage of this method is that the Fe^{3+}/Fe^{2+} system is catalytic and reaction (3) is propagated from Fe^{2+} regeneration, mainly by reduction of Fe^{3+} at the cathode [21]. However, a part of generated $^\bullet$OH is wasted by non-oxidizing reactions, for example, with Fe^{2+} and H_2O_2 or its direct recombination to hydrogen peroxide [32,33]:

$$Fe^{2+} + {}^\bullet OH \rightarrow Fe^{3+} + OH^- \quad (4)$$

$$H_2O_2 + {}^\bullet OH \rightarrow HO_2^\bullet + H_2O \quad (5)$$

$$2{}^\bullet OH \rightarrow H_2O_2 \quad (6)$$

In the photoelectro-Fenton process, the treated solution is illuminated with UV light, which can also act as catalyst to favor: (i) the photodecomposition of complexes of Fe^{3+} with generated carboxylic acids [23,25,30,34] and/or (ii) the regeneration of more Fe^{2+} with additional production of $^\bullet$OH from photoreduction of $Fe(OH)^{2+}$, the predominant Fe^{3+} species in acid medium [32]:

$$Fe(OH)^{2+} + h\nu \rightarrow Fe^{2+} + {}^\bullet OH \quad (7)$$

This paper reports a comparative study on the degradation of clofibric acid by electro-Fenton and photoelectro-Fenton using an undivided electrolytic cell with a BDD anode and an O_2-diffusion cathode to electrogenerate continuously H_2O_2 from reaction (2). Both AEOPs were tested with metabolite solutions containing a low content of 0.05 M Na_2SO_4 as background electrolyte and 1.0 mM Fe^{2+} as catalyst at pH 3.0, near the optimum pH of 2.8 for Fenton's reaction (3) [32]. For these methods, organic pollutants are expected to be mainly oxidized by BDD($^\bullet$OH) and $^\bullet$OH formed from reactions (1) and (3), respectively, although parallel reactions with weaker oxidants such as electrogenerated H_2O_2, as well as peroxodisulfate ion [18], ozone [18] and ferrate ion [35] also produced at the BDD anode, are possible in much less extent. Photoelectro-Fenton was performed by irradiating the solution with UVA light. Comparative treatments by anodic oxidation without and with UVA irradiation were also made to assess the higher oxidation power of electro-Fenton and photoelectro-Fenton. The influence of current density and metabolite concentration on the degradation rate and mineralization current efficiency of these AEOPs was investigated. The decay kinetics of clofibric acid in each method was determined. The evolution of identified aromatic products and carboxylic acids was followed by chromatographic techniques to clarify their pathways in the different oxidation processes.

2. Experimental

Clofibric acid, 4-chlorophenol, hydroquinone, *p*-benzoquinone, 2-hydroxyisobutyric acid, tartronic acid, maleic acid, fumaric acid, formic acid and oxalic acid were either reagent or analytical grade from Sigma–Aldrich, Merck, Panreac and Avocado. 4-Chlorocatechol was synthesized by chlorination of pyrocatechol with SO_2Cl_2 [23]. Anhydrous sodium sulfate and heptahydrated ferrous sulfate were analytical grade from Fluka. Solutions were prepared with high-purity water obtained from a Millipore Milli-Q system (resistivity >18 MΩ cm at 25 °C) and their pH was adjusted to 3.0 with analytical grade sulfuric acid from Merck. Other chemicals and organic solvents were either HPLC or analytical grade from Panreac.

The solution pH was determined with a Crison 2000 pH-meter. Aliquots withdrawn from treated solutions were filtered with Whatman 0.45 μm PTFE filters before analysis. The degradation of clofibric acid solutions was monitored from the removal of their total organic carbon (TOC), measured on a Shimadzu VCSN TOC analyzer. Reproducible values were obtained using the standard non-purgeable organic carbon method. From these results, the mineralization current efficiency (MCE) for each treated solution at a given

electrolysis time was calculated from the following equation:

$$\mathrm{MCE} = \frac{\Delta(\mathrm{TOC})_{\mathrm{exp}}}{\Delta(\mathrm{TOC})_{\mathrm{theor}}} \times 100 \quad (8)$$

where $\Delta(\mathrm{TOC})_{\mathrm{exp}}$ is the experimental TOC decay and $\Delta(\mathrm{TOC})_{\mathrm{theor}}$ is the theoretically calculated TOC removal assuming that the applied electrical charge (=current × time) is only consumed in the mineralization process of clofibric acid.

The concentration of chloride ion in treated solutions was determined by ion chromatography with a Shimadzu 10Avp HPLC chromatograph fitted with a Shim-Pack IC-A1S, 100 mm × 4.6 mm (i.d.), anion column at 40 °C and coupled with a Shimadzu CDD 10Avp conductivity detector. A mixture of 2.5 mM phtalic acid and 2.4 mM tris(hydroxymethyl)aminomethane of pH 4.0 at 1.5 ml min^{-1} was used as mobile phase for this analysis. Aromatic products were identified by gas chromatography–mass spectrometry (GC–MS) using a Hewlett-Packard 5890 Series II gas chromatograph fitted with a HP-5 0.25 μm, 30 m × 0.25 mm (i.d.), column, and a Hewlett-Packard 5989A mass spectrophotometer operating in EI mode at 70 eV and 290 °C. The metabolite decay and the time-course of its aromatic products were followed by reversed-phase HPLC chromatography using a Waters 600 high-performance liquid chromatograph fitted with a Spherisorb ODS2 5 μm, 150 mm × 4.6 mm (i.d.), column at room temperature, coupled with a Waters 996 photodiode array detector, and circulating a 50:47:3 (v/v/v) methanol/phosphate buffer (pH 2.5)/pentanol mixture at 1.0 ml min^{-1} as mobile phase. For each product, this detector was selected at the maximum wavelength of its UV-absorption band. Carboxylic acids were identified by ion-exclusion chromatography using the above HPLC chromatograph fitted with a Bio-Rad Aminex HPX 87H, 300 mm × 7.8 mm (i.d.), column at 35 °C. For these measurements, the photodiode detector was selected at 210 nm and the mobile phase was 4 mM H_2SO_4 at 0.6 ml min^{-1}.

All electrolyses were conducted in an open, cylindrical, undivided and thermostated cell containing 100 ml of solution vigorously stirred with a magnetic bar. The anode was a 3 cm^2 BDD thin-film deposited on conductive single crystal p-type Si (1 0 0) wafers from CSEM and the cathode was a 3 cm^2 carbon-PTFE electrode from E-TEK, which was fed with pure O_2 at 12 ml min^{-1} to generate continuously H_2O_2 from reaction (2). The setup of the electrolytic system and the characteristics of the O_2-diffusion cathode have been described elsewhere [23,25]. Experiments were made at a constant current density (j) of 33, 100 and 150 mA cm^{-2}, supplied by an Amel 2053 potentiostat–galvanostat. Electro-Fenton and photoelectro-Fenton treatments were carried out with solutions containing 0.05 M Na_2SO_4 as background electrolyte and 1.0 mM Fe^{2+} as catalyst of pH 3.0 at 35.0 °C, which were found as optimum conditions for the degradation of other aromatics in the cell used [23,25]. The latter method became operative when the solution was irradiated with UVA light of λ_{max} = 360 nm emitted by a Philips 6 W fluorescent black light blue tube, yielding a photoionization energy input to the solution of 140 μW cm^{-2}, as detected with a NRC 820 laser power meter working at 514 nm. Comparative anodic oxidation treatments without catalyst Fe^{2+} were performed in the absence and presence of UVA irradiation at 100 mA cm^{-2}.

3. Results and discussion

3.1. Comparative degradation of clofibric acid

Comparative treatments were made for solutions containing 179 mg l^{-1} clofibric acid (equivalent to 100 mg l^{-1} TOC) of pH 3.0 at 100 mA cm^{-2}. In these trials the solution pH did not practically vary, reaching final values of 2.8–2.9. The change in solution TOC with applied specific charge (Q, in Ah l^{-1}) for anodic oxidation without and with UVA irradiation, electro-Fenton and photoelectro-Fenton is depicted in Fig. 1. As can be seen, total degradation (>97% TOC removal) is attained in all cases, although the time required for overall mineralization depends on the method tested. Both anodic oxidation methods lead to a slow, but similar, TOC decay up to yield total mineralization at Q = 18 Ah l^{-1}, i.e., after 6 h of both treatments. This behavior indicates that all organics are destroyed by the oxidant BDD($^{\bullet}$OH) formed at the anode surface from reaction (1), without significant photodecomposition by UVA light, at least of final products. Fig. 1 evidences that the degradation rate (the change of TOC with time) is strongly enhanced using both AEOPs due to the catalytic action of the Fe^{3+}/Fe^{2+} system combined with UVA light when the solution is simultaneously irradiated. The significant acceleration of the destruction of organic pollutants in the early stages of the electro-Fenton process can be explained by their quicker reaction with the great amount of $^{\bullet}$OH formed from Fenton's reaction (3). For this AEOP, however, the rate in TOC decay gradually falls at longer electrolysis time, probably due to the formation of complexes of Fe^{3+} with final carboxylic acids that are hardly oxidized, and the solution is decontaminated after

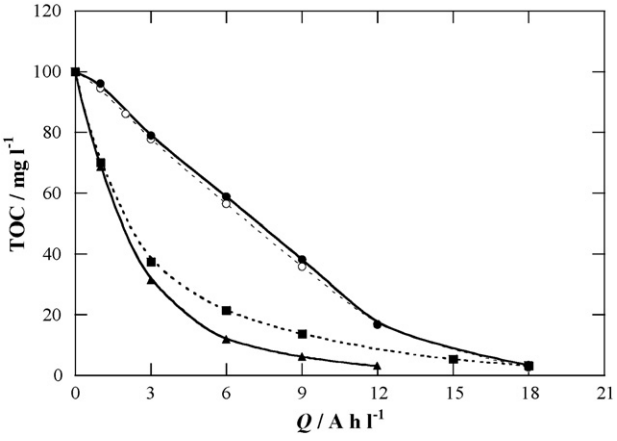

Fig. 1. TOC removal with specific charge for the degradation of 100 ml solutions containing 179 mg l^{-1} clofibric acid and 0.05 M Na_2SO_4 of pH 3.0 at 100 mA cm^{-2} and at 35.0 °C using an undivided cell with a 3 cm^2 BDD anode and a 3 cm^2 carbon-PTFE cathode fed with pure O_2 at 12 ml min^{-1}. Method: (○) anodic oxidation with electrogenerated H_2O_2, (●) anodic oxidation with electrogenerated H_2O_2 under a 6 W UVA irradiation with λ_{max} = 360 nm, (■) electro-Fenton with 1.0 mM Fe^{2+} and (▲) photoelectro-Fenton with 1.0 mM Fe^{2+} and UVA light.

about 6 h of electrolysis, that is, at similar time to that needed for both anodic oxidation treatments. In contrast, TOC is much more rapidly removed by photoelectro-Fenton, where total mineralization is achieved at $Q = 12$ Ah l^{-1} (4 h). The increase in mineralization rate in photoelectro-Fenton can be related to: (i) the parallel photodegradation of complexes of Fe^{3+} with final carboxylic acids and/or (ii) the enhanced generation of $^{\bullet}OH$ due to additional photoreduction of $Fe(OH)^{2+}$ from reaction (7).

The above comparative study shows that photoelectro-Fenton is the method with highest oxidation power due to large enhancement of the destruction of final products by UVA light, then being the best AEOP for the treatment of wastewaters containing clofibric acid. Electro-Fenton also yields much faster degradation than anodic oxidation, but its oxidation power drops significantly at the end of electrolysis because final products are difficultly oxidized by $^{\bullet}OH$.

The influence of current density and clofibric acid concentration on the oxidizing ability of the above electro-Fenton and photoelectro-Fenton processes was explored. It was found that these experimental parameters showed the same trends in both AEOPs, as expected if they mainly affect the behavior of the electrolytic system. These effects are depicted in Fig. 2a and b for electro-Fenton in which they were more clearly observed due to its lower oxidation power. Thus, Fig. 2a shows that when j increases from 33 to 150 mA cm^{-2}, the specific charge for total decontamination of 179 mg l^{-1} of clofibric acid rises from 12 to 22 Ah l^{-1}, but the time needed for overall mineralization drops from 12 to about 5 h since the degradation rate is strongly enhanced. This latter tendency can be accounted for by the faster destruction of all pollutants due to the greater production of BDD($^{\bullet}OH$) from reaction (1) and of $^{\bullet}OH$ from Fenton's reaction (3) as j increases, because more H_2O_2 is generated at the O_2-diffusion cathode from reaction (2) [25] and then, its reaction with Fe^{2+} becomes faster. However, the increase in Q for total decontamination when j rises suggests a lower amount of reactive BDD($^{\bullet}OH$) and $^{\bullet}OH$. That means that a higher proportion of both oxidants is progressively wasted by their non-oxidizing reactions since they take place in larger extent. These reactions involve, for example, the anodic oxidation of BDD($^{\bullet}OH$) to O_2 and reactions (4)–(6) for $^{\bullet}OH$. Moreover, increasing j can accelerate the formation of weaker oxidants such as peroxodisulfate ion [18], ozone [18] and chlorine (see Section 3.2) that also reduce the relative proportion of BDD($^{\bullet}OH$) adsorbed at the anode. On the other hand, Fig. 2b shows that at 100 mA cm^{-2} overall mineralization is achieved with decreasing consumption of 24 Ah l^{-1} (8 h), 21 Ah l^{-1} (7 h), 18 Ah l^{-1} (6 h) and 12 Ah l^{-1} (4 h) starting from 557 (close to saturation), 358, 179 and 89 mg l^{-1} of the metabolite, respectively, as expected if lower relative amount of organic matter is destroyed in solution. These results also evidence the removal of more TOC at a given time with rising initial pollutant content. As an example, at 2 h of electrolysis ($Q = 6$ Ah l^{-1}) the TOC of the above solutions is reduced by 231, 150, 70 and 39 mg l^{-1}. Since the same quantity of BDD($^{\bullet}OH$) and $^{\bullet}OH$ is expected to be produced from reactions (1) and (3) in these trials carried out at 100 mA cm^{-2}, it can be assumed that their parallel non-oxidizing reactions occur in less proportion with rising metabolite concentration. This favors the reaction of more amounts of both kinds of hydroxyl radicals with organics, thus raising the degradation rate of the process. All these findings allow establishing that the oxidation power of AEOPs, corresponding to their degradation rate, increases with increasing current density and initial substrate concentration.

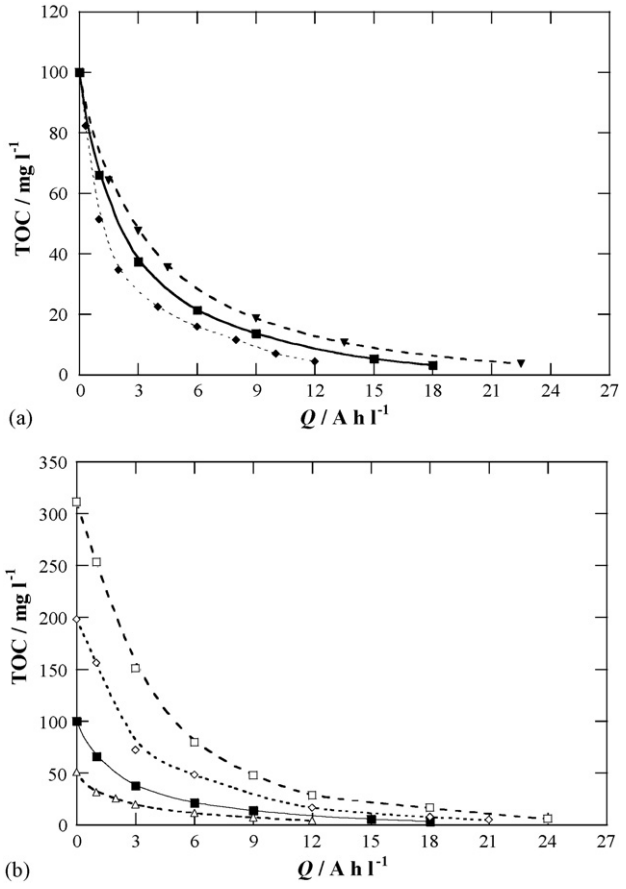

Fig. 2. Effect of experimental parameters on TOC abatement vs. specific charge for the treatment of 100 ml of clofibric acid solutions of pH 3.0 at 35.0 °C by electro-Fenton with a BDD anode and 1.0 mM Fe^{2+}. In plot (a), metabolite concentration: 179 mg l^{-1}; current density: (◆) 33, (■) 100 and (▼) 150 mA cm^{-2}. In plot (b), metabolite concentration: (□) 557 (close to saturation), (◇) 358, (■) 179 and (△) 89 mg l^{-1}; current density: 100 mA cm^{-2}.

3.2. Mineralization current efficiency

It is well-known that reaction of chloroaromatics with hydroxyl radical leads to the release of chloride ion [16,23,26]. This point was confirmed for clofibric acid by recording the ion chromatograms of all treated solutions, which only displayed a defined peak at a retention time (t_r) of 2.3 min related to Cl^- ion. The formation of ClO_3^- and ClO_4^- ions was discarded since they were not detected in these chromatograms. The evolution of Cl^- concentration during the degradation of 179 mg l^{-1} of metabolite by anodic oxidation with electrogenerated H_2O_2 and the two AEOPs at 100 mA cm^{-2} is presented in Fig. 3. As can be seen, this ion is accumulated and completely removed in 300–360 min in all cases, after reaching

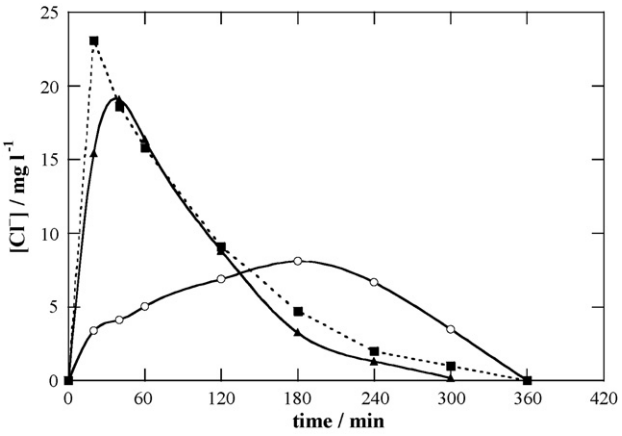

Fig. 3. Concentration of chloride ion accumulated during the treatment of 100 ml of 179 mg l^{-1} clofibric acid solutions of pH 3.0 at 100 mA cm^{-2} and at 35.0 °C using a BDD anode and electrogenerated H_2O_2 by: (○) anodic oxidation, (■) electro-Fenton and (▲) photoelectro-Fenton.

a maximum concentration of about 8 mg l^{-1} at 180 min of anodic oxidation, 23 mg l^{-1} at 20 min of electro-Fenton and 19 mg l^{-1} at 40 min of photoelectro-Fenton, corresponding to 27, 78 and 64% of the initial chlorine content in solution (29.5 mg l^{-1}). The slow accumulation of Cl^- in the former method confirms the slow reaction of chloro-organics with BDD($^\bullet$OH), whereas its much faster release at the early stages of both AEOPs corroborates the quick destruction of these pollutants with $^\bullet$OH. The gradual destruction of this ion when electrolysis is prolonged can be explained by its slow oxidation to Cl_2 on BDD, as reported by Kraft et al. [16].

The above findings allow concluding that the mineralization of clofibric acid involves its conversion into CO_2 and Cl^- as primary ion. This reaction can be written as follows:

$$C_{10}H_{11}ClO_3 + 17H_2O \rightarrow 10CO_2 + Cl^- + 45H^+ + 44e^- \quad (9)$$

Reaction (9) was then used to calculate the value of $\Delta(TOC)_{theor}$ for each treated solution at chosen electrolysis times and from these data, the corresponding efficiency by means of Eq. (8).

Fig. 4a presents the MCE values determined for the trials reported in Fig. 1. An increase in efficiency with increasing the oxidation power of the method can be observed. Thus, the two less potent anodic oxidation processes possess a similar, small and practically constant MCE value of about 7%, suggesting that most organics are mineralized at the same rate by BDD($^\bullet$OH) along electrolysis without significant role of UVA light. In contrast, this parameter attains a much higher value for electro-Fenton and photoelectro-Fenton, although the latter procedure with highest oxidation power is the most efficient because of the parallel photodecomposition of some final products. Note that 33 and 35% efficiencies are found after 20 min of these AEOPs, respectively, confirming that organics are more quickly mineralized with $^\bullet$OH than with BDD($^\bullet$OH). At longer time, a dramatic drop in MCE takes place in both cases due to the generation of final products such as complexes of Fe^{3+} with carboxylic acids that are more difficultly destroyed by both oxidants and/or UVA light.

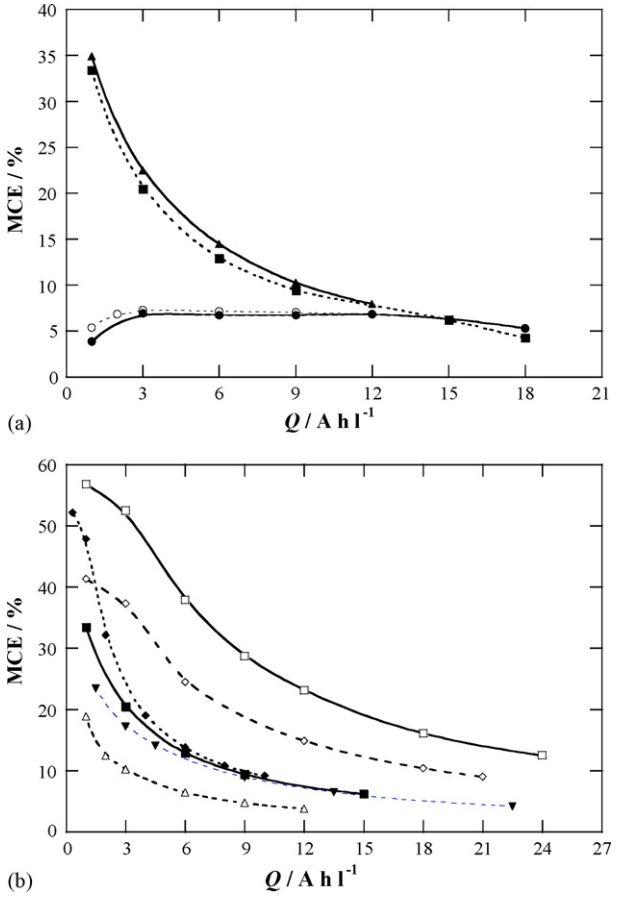

Fig. 4. Mineralization current efficiency calculated from Eq. (8) vs. specific charge. Plot (a) corresponds to the experiments shown in Fig. 1 and plot (b) to those reported in Fig. 2a and b.

Fig. 4b illustrates the effect of current density and clofibric acid concentration reported in Fig. 2a and b on the efficiency of AEOPs as a function of specific charge. A gradual drop in MCE, at least up to 6 Ah l^{-1}, can be observed when j increases from 33 to 150 mA cm^{-2}. This trend could seem contradictory to the fact that rising j causes the increase in degradation rate due to the production of more amounts of reactive BDD($^\bullet$OH) and $^\bullet$OH, as pointed out above. The concomitant loss in efficiency under these conditions can be associated with the larger waste of both oxidants in faster parallel non-oxidizing reactions giving rise to lower amounts of them with ability to destroy organics and hence, favoring the consumption of more ineffective specific charge. Fig. 4b also evidences a gradual increase in efficiency of AEOPs with rising metabolite concentration, in agreement with the higher degradation rate found in these trials. This confirms the removal of greater amounts of pollutants with BDD($^\bullet$OH) and $^\bullet$OH, because their competitive non-oxidizing reactions become less significant.

3.3. Kinetics of clofibric acid decay

The decay of the metabolite in the different electrochemical methods was followed by reversed-phase HPLC chromatography, where it exhibited a well-defined peak at t_r = 7.9 min. A

previous experiment carried out by adding 20 mM H_2O_2 to a 179 mg l^{-1} clofibric acid solution of pH 3.0 showed that the content of this compound remained unchanged, indicating that it cannot react directly with electrogenerated H_2O_2 in the electrolytic systems.

The comparative kinetics of the removal of clofibric acid with generated strong oxidizing agents (mainly BDD($^\bullet$OH) and/or $^\bullet$OH) was determined from the treatment of 179 mg l^{-1} metabolite solutions at 100 mA cm^{-2}. Fig. 5a shows that clofibric acid concentration undergoes a similar fall by anodic oxidation without and with UVA illumination, disappearing in 360 min in both cases, a time similar to that needed for its total mineralization (see Fig. 1). This confirms that this compound is mainly oxidized by BDD($^\bullet$OH) from reaction (1), without direct photolysis by UVA light. The above concentration decays were well-fitted to a pseudo-first-order equation, as can be seen in the inset panel of Fig. 5a. From this kinetic analysis, a pseudo-first-order rate constant (k) of 1.58×10^{-4} s^{-1} (square regression coefficient (R^2) = 0.992) and 1.85×10^{-4} s^{-1} (R^2 = 0.993) is found for anodic oxidation in the absence and presence of UVA light, respectively. This behavior suggests

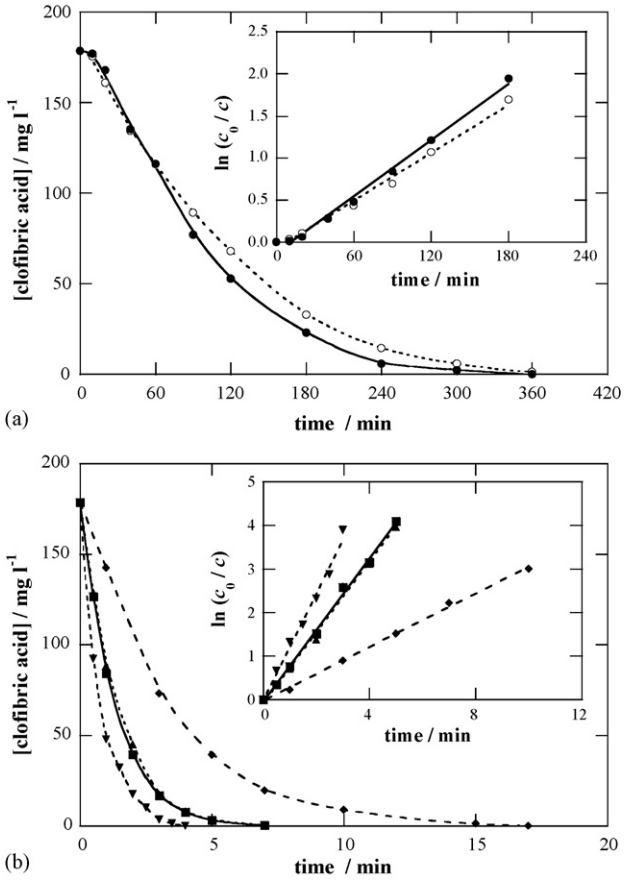

Fig. 5. Time-course of clofibric acid concentration during the degradation of 100 ml of 179 mg l^{-1} metabolite solutions of pH 3.0 at 35.0 °C with a BDD anode and electrogenerated H_2O_2. Plot (a): (○) anodic oxidation and (●) anodic oxidation with UVA light at 100 mA cm^{-2}. Plot (b): electro-Fenton at (◆) 33, (■) 100 and (▼) 150 mA cm^{-2} and (▲) photoelectro-Fenton at 100 mA cm^{-2}. The inset panels show the corresponding kinetic analysis assuming a pseudo-first-order reaction for clofibric acid.

that a steady BDD($^\bullet$OH) concentration reacts with the metabolite along electrolysis.

On the other hand, Fig. 5b evidences a much quicker and similar abatement of the metabolite under comparable electro-Fenton and photoelectro-Fenton treatments, being completely removed in 7 min, as expected if it reacts with a much greater amount of oxidant $^\bullet$OH formed from Fenton's reaction (3). The inset panel of Fig. 5b shows that the kinetic analysis of these data also agrees with a pseudo-first-order reaction, giving the same k-value of 1.35×10^{-2} s^{-1} (R^2 = 0.993). This allows concluding that $^\bullet$OH is produced in insignificant quantity by reaction (7) under UVA irradiation and hence, the higher TOC removal found for photoelectro-Fenton in comparison to electro-Fenton (see Fig. 1) can be ascribed to the fast parallel photodecomposition of complexes of Fe^{3+} with final carboxylic acids, as will be discussed below.

The effect of current density on the decay kinetics of this compound was further explored for the electro-Fenton treatment. As can be seen in Fig. 5b, increasing k-values of 5.10×10^{-3} s^{-1} (R^2 = 0.991), 1.35×10^{-2} s^{-1} (R^2 = 0.993) and 2.04×10^{-2} s^{-1} (R^2 = 0.992) are found for j values of 33, 100 and 150 mA cm^{-2}, respectively. This trend confirms a higher $^\bullet$OH production in the medium from Fenton's reaction (3) when j rises, due to the concomitant accumulation of more electrogenerated H_2O_2 from reaction (2) [25].

3.4. Identification and evolution of intermediates

A 179 mg l^{-1} clofibric acid solution of pH 3.0 was treated by electro-Fenton at 100 mA cm^{-2} for 2 min and its organic components were extracted with 45 ml of CH_2Cl_2 in three times. The collected organic solution was dried with Na_2SO_4, filtered and its volume reduced to 2 ml to concentrate the remaining aromatics to be analyzed by GC–MS. The MS spectrum showed peaks related to stable aromatics such as 4-chlorophenol (m/z = 128 (100, M^+), 130 (33, $(M + 2)^+$)) at t_r = 17.0 min, hydroquinone (m/z = 108 (100, M^+)) at t_r = 21.5 min, 4-chlorocatechol (m/z = 144 (100, M^+), 146 (33, $(M + 2)^+$)) at t_r = 18.2 min and p-benzoquinone (m/z = 110 (53, M^+)) at t_r = 4.1 min. These products were confirmed in the reversed-phase HPLC chromatograms of electrolyzed solutions, which exhibited well-defined peaks corresponding to 4-chlorophenol at t_r = 5.0 min, 4-chlorocatecol at t_r = 3.1 min and p-benzoquinone at t_r = 2.0 min. These peaks were unequivocally identified by comparing their t_r-values and UV–vis spectra, measured on the photodiode detector, with those of pure compounds. However, only traces of hydroquinone were detected by this technique in all cases, as expected if it is very quickly converted into p-benzoquinone by all oxidizing agents.

The evolution of aromatic intermediates during the different treatments of 179 mg l^{-1} metabolite solutions at 100 mA cm^{-2} is presented in Fig. 6. As can be seen in Fig. 6a, 4-chlorophenol is largely produced in all cases and persists long time, up to 360 min, in both anodic oxidation processes, but it is removed very rapidly, for 7–8 min, in electro-Fenton and photoelectro-Fenton (see the inset panel of Fig. 6a). Comparison of results of Figs. 6a and 5 evidences that in each method this primary

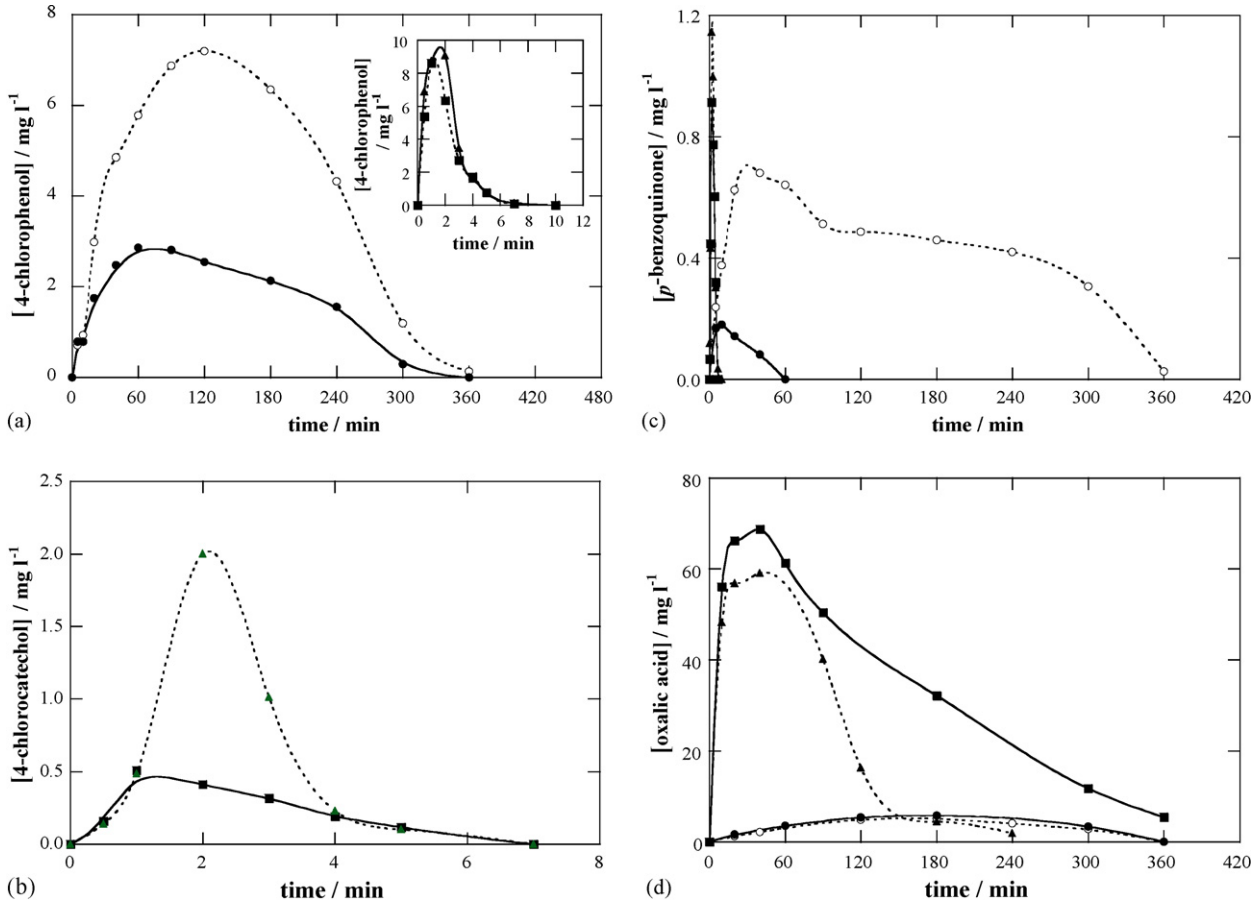

Fig. 6. Evolution of the concentration of selected intermediates during the mineralization of 100 ml of 179 mg l^{-1} clofibric acid solutions of pH 3.0 at 100 mA cm^{-2} and at 35.0 °C with a BDD anode and electrogenerated H_2O_2. Plots correspond to: (a) 4-chlorophenol, (b) 4-chlorocatechol, (c) *p*-benzoquinone and (d) oxalic acid. Method: (○) anodic oxidation, (●) anodic oxidation with UVA light, (■) electro-Fenton and (▲) photoelectro-Fenton.

product disappears at the same time as the initial pollutant. In contrast, Fig. 6b shows that 4-chlorocatechol is accumulated in much smaller extent in the two latter AEOPs, disappearing in 7 min. The same removal time is found for *p*-benzoquinone in electro-Fenton and photoelectro-Fenton, although it persists for 60 and 360 min in anodic oxidation with and without UVA irradiation, respectively (see Fig. 6c). These findings suggest the parallel quick photolysis of *p*-benzoquinone by UVA light, which it is not observed in photoelectro-Fenton because it reacts much more quickly with $^{\bullet}OH$.

From the above results, a general reaction sequence for the initial degradation of clofibric acid is proposed in Fig. 7, where pollutants can react with BDD($^{\bullet}OH$) formed at the anode surface from reaction (1) and/or with $^{\bullet}OH$ produced from Fenton's reaction (3) in the medium. The process is initiated by the breaking of the C(1)–O bond of clofibric acid by both oxidants to yield 4-chlorophenol and 2-hydroxyisobutyric acid as primary products. Further attack of BDD($^{\bullet}OH$) and $^{\bullet}OH$ on the C(4)-position of 4-chlorophenol gives hydroquinone, with loss of Cl^- ion, which is then oxidized to *p*-benzoquinone. Parallel hydroxylation of 4-chlorophenol only by attack of $^{\bullet}OH$ on its C(2)-position leads to 4-chlorocatechol. The subsequent oxidation of the latter product, with release of Cl^-, and *p*-benzoquinone (not shown in Fig. 7) can cause the opening of their benzenic rings to yield different carboxylic acids. The formation of such products was confirmed from analysis of degraded solutions by ion-exclusion HPLC chromatography.

Ion-exclusion chromatograms of solutions treated by the two anodic oxidation methods displayed peaks ascribed to small contents of generated carboxylic acids such as 2-hydroxyisobutyric at t_r = 12.6 min, tartronic at t_r = 7.7 min, maleic at t_r = 8.1 min, fumaric at t_r = 16.1 min, formic at t_r = 14.0 min and oxalic at t_r = 6.6 min. Tartronic, maleic, fumaric and formic acids come from the oxidation of the aryl moiety of aromatics [26,29,31], whereas 2-hydroxyisobutyric acid is expected to be released in the early stages of the degradation process when 4-chlorophenol is formed (see Fig. 7). All these acids, except oxalic acid, were undetected or detected as traces for short time in electro-Fenton and photoelectro-Fenton. Oxalic acid was accumulated in large extent and persisted up to the end of the mineralization in both processes. This ultimate acid formed from the independent oxidation of the precedent longer-chain carboxylic acids, as well as formic acid, are directly converted into CO_2 [17,29,31].

Fig. 6d presents the time-course of oxalic acid concentration during all treatments. In both anodic oxidation methods this acid is formed and destroyed at similar rate, reaching 5–6 mg l^{-1} as maximum at 180 min and disappearing in

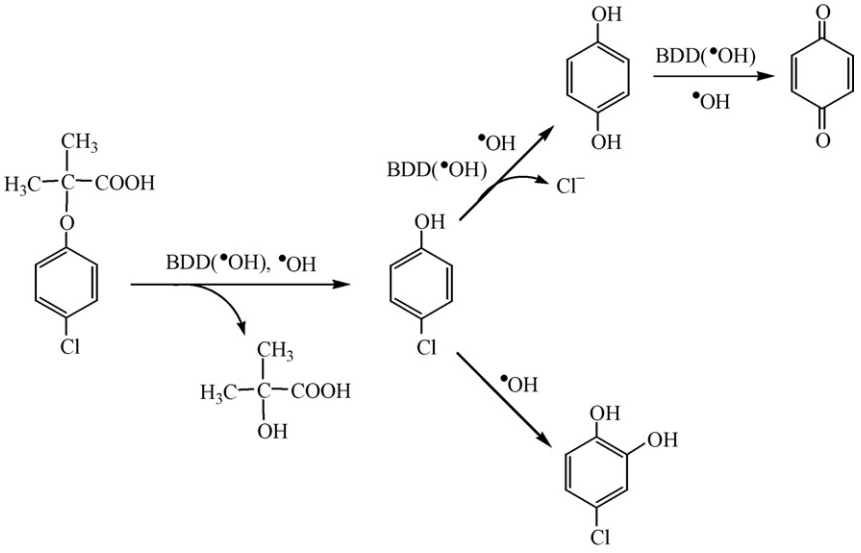

Fig. 7. Proposed reaction sequence for the initial degradation of clofibric acid with a BDD anode and electrogenerated H_2O_2 by anodic oxidation, electro-Fenton with Fe^{2+} and photoelectro-Fenton with Fe^{2+} and UVA light. The oxidant hydroxyl radical is denoted as BDD(•OH) or •OH when it is formed at the BDD anode surface or from Fenton's reaction, respectively.

360 min, just when the initial substrate is completely removed (see Fig. 5a) and the solution is totally decontaminated (see Fig. 1). This confirms the simultaneous destruction of clofibric acid and most of its products with BDD(•OH) in these processes, in agreement with the constant efficiency found during degradation (see Fig. 4a). In contrast, oxalic acid reaches high contents of 68 and 59 mg l^{-1} after 40 min of electro-Fenton and photoelectro-Fenton, respectively, due to the very quick oxidation of precedent organics with •OH formed from Fenton's reaction (3). Nevertheless, it is completely removed in 240 min by photoelectro-Fenton, just when the solution is totally decontaminated (see Fig. 1), still remaining about 6 mg l^{-1} (less than 1.5 mg l^{-1} of TOC) in solution after 360 min of electro-Fenton. Since in these AEOPs a large amount of Fe^{3+} is formed in the medium from reactions (3) and (4), oxalic acid is really expected to be present in the form of Fe^{3+}–oxalato complexes, which cannot be oxidized by •OH in the medium [23,29,33]. Our results indicate that these complexes are slowly mineralized in electro-Fenton with a BDD anode and even more quickly photodecomposed by UVA irradiation in photoelectro-Fenton.

According to these considerations, Fig. 8 shows a proposed degradation pathway for oxalic acid under the present

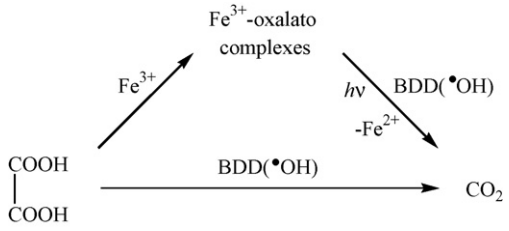

Fig. 8. Proposed reaction pathways for oxalic acid mineralization with a BDD anode and electrogenerated H_2O_2 by anodic oxidation, electro-Fenton with Fe^{2+} and photoelectro-Fenton with Fe^{2+} and UVA light.

experimental conditions. This acid is oxidized to CO_2 with BDD(•OH) at the anode surface either directly in both anodic oxidation treatments or as Fe^{3+}–oxalato complexes in electro-Fenton. The latter complexes also undergo a parallel quick photodecarboxylation under the action of UVA light in photoelectro-Fenton, with regeneration of Fe^{2+} as proposed by Zuo and Hoigné [34]. This photolytic reaction explains the fastest degradation rate and highest efficiency of photoelectro-Fenton. The fact that oxalic acid is still detected after 6 h of electro-Fenton, while it is removed at the same time for anodic oxidation, suggests a slower reaction of BDD(•OH) with its Fe^{3+} complexes that causes the decay in oxidation power of this AEOP at long electrolysis time.

4. Conclusions

It is demonstrated that AEOPs such as electro-Fenton with Fe^{2+} and photoelectro-Fenton with Fe^{2+} and UVA light, both with a BDD anode, yield an efficient and complete degradation of aqueous solutions of clofibric acid up to saturation at pH 3.0. The efficiency of both methods increases with rising metabolite concentration and with decreasing current density. Comparative treatments by anodic oxidation are much slower, confirming the high production of •OH from Fenton's reaction (3) in the above AEOPs. In all methods Cl^- is released and totally oxidized to Cl_2 on BDD. The clofibric acid decay always follows a pseudo-first-order kinetics. This compound is hydroxylated to yield 4-chlorophenol, which is further oxidized either to *p*-benzoquinone via hydroquinone or to 4-chlorocatechol. These products are subsequently degraded to tartronic, maleic and fumaric acids, which are quickly converted into oxalic acid. The latter acid is also obtained from the oxidation of 2-hydroxyisobutyric acid, initially generated when 4-chlorophenol is formed. Formic acid also generated in the degradation path is rapidly converted into CO_2. The ultimate product oxalic acid is then transformed into

CO_2 on BDD either directly in anodic oxidation or as Fe^{3+}–oxalato complexes in electro-Fenton. The parallel quick photolysis of these complexes by UVA light in photoelectro-Fenton explains the fastest degradation rate and highest efficiency of this method, which appears to be the best AEOP for the treatment of wastewaters containing clofibric acid.

Acknowledgements

Financial support from MEC (Ministerio de Educación y Ciencia, Spain) under project CTQ2004-01954/BQU and the grant awarded to I. Sirés from DURSI (Departament d'Universitats, Recerca i Societat de la Informació, Generalitat de Catalunya) to do this work are acknowledged.

References

[1] T. Heberer, H.J. Stan, Int. J. Environ. Anal. Chem. 67 (1997) 113–124.
[2] H.R. Buser, M.D. Muller, N. Theobald, Environ. Sci. Technol. 32 (1998) 188–192.
[3] K. Kümmerer (Ed.), Pharmaceuticals in the Environment. Sources, Fate and Risks, Springer, Berlin, 2001.
[4] D.W. Kolpin, E.T. Furlong, M.T. Meyer, E.M. Thurman, S.D. Zaugg, L.B. Barber, Environ. Sci. Technol. 36 (2002) 1202–1211.
[5] T.A. Ternes, M. Meisenheimer, D. McDowell, F. Sacher, H.J. Brauch, B. Haist-Gulde, G. Preuss, U. Wilme, N. Zulei-Seibert, Environ. Sci. Technol. 36 (2002) 3855–3863.
[6] C. Tixier, H.P. Singer, S. Oellers, S.R. Müller, Environ. Sci. Technol. 37 (2003) 1061–1068.
[7] J.L. Packer, J.J. Werner, D.E. Latch, K. McNeill, W.A. Arnold, Aquat. Sci. 65 (2003) 342–351.
[8] J.P. Bound, N. Vaulvaulis, Chemosphere 56 (2004) 1143–1155.
[9] A. Tauxe-Wuersch, L.F. De Alencastro, D. Grandjean, J. Tarradellas, Water Res. 39 (2005) 1761–1772.
[10] J.P. Emblidge, M.E. DeLorenzo, Environ. Res. 100 (2006) 216–226.
[11] R. Andreozzi, V. Caprio, R. Marotta, A. Radovnikovic, J. Hazard. Mater. B103 (2003) 233–246.
[12] T. Doll, F.H. Frimmel, Water Res. 38 (2004) 955–964.
[13] I. Sirés, P.L. Cabot, F. Centellas, J.A. Garrido, R.M. Rodríguez, C. Arias, E. Brillas, Electrochim. Acta 52 (2006) 75–85.
[14] M. Panizza, P.A. Michaud, G. Cerisola, Ch. Comninellis, J. Electroanal. Chem. 507 (2001) 206–214.
[15] B. Marselli, J. García-Gomez, P.A. Michaud, M.A. Rodrigo, Ch. Comninellis, J. Electrochem. Soc. 150 (2003) D79–D83.
[16] A. Kraft, M. Stadelmann, M. Blaschke, J. Hazard. Mater. B 103 (2003) 247–261.
[17] C.A. Martinez-Huitle, S. Ferro, A. De Battisti, Electrochim. Acta 49 (2004) 4027–4034.
[18] M. Panizza, G. Cerisola, Electrochim. Acta 51 (2005) 191–199.
[19] A. Alverez-Gallegos, D. Pletcher, Electrochim. Acta 44 (1999) 2483–2492.
[20] T. Harrington, D. Pletcher, J. Electrochem. Soc. 146 (1999) 2983–2989.
[21] M.A. Oturan, J.J. Aaron, N. Oturan, J. Pinson, Pestic. Sci. 55 (1999) 558–562.
[22] M.A. Oturan, J. Appl. Electrochem. 30 (2000) 475–482.
[23] B. Boye, M.M. Dieng, E. Brillas, Environ. Sci. Technol. 36 (2002) 3030–3035.
[24] B. Gözmen, M.A. Oturan, N. Oturan, O. Erbatur, Environ. Sci. Technol. 37 (2003) 3716–3723.
[25] E. Brillas, M.A. Baños, S. Camps, C. Arias, P.L. Cabot, J.A. Garrido, R.M. Rodríguez, New J. Chem. 28 (2004) 314–322.
[26] E. Brillas, B. Boye, I. Sirés, J.A. Garrido, R.M. Rodríguez, C. Arias, P.L. Cabot, Ch. Comninellis, Electrochim. Acta 49 (2004) 4487–4496.
[27] K. Hanna, S. Chiron, M.A. Oturan, Water Res. 39 (2005) 2763–2773.
[28] A. Wang, J. Qu, J. Ru, H. Liu, J. Ge, Dyes Pigments 65 (2005) 227–233.
[29] I. Sirés, J.A. Garrido, R.M. Rodríguez, P.L. Cabot, F. Centellas, C. Arias, E. Brillas, J. Electrochem. Soc. 153 (2006) D1–D9.
[30] S. Irmak, H.I. Yavuz, O. Erbatur, Appl. Catal. B: Environ. 63 (2006) 243–248.
[31] C. Flox, S. Ammar, C. Arias, E. Brillas, A.V. Vargas-Zavala, R. Abdelhedi, Appl. Catal. B: Environ. 67 (2006) 93–104.
[32] Y. Sun, J.J. Pignatello, Environ. Sci. Technol. 27 (1993) 304–310.
[33] G.U. Buxton, C.L. Greenstock, W.P. Helman, A.B. Ross, J. Phys. Chem. Data Ref. 17 (1988) 513–886.
[34] Y. Zuo, J. Hoigné, Environ. Sci. Technol. 26 (1992) 1014–1022.
[35] J. Lee, D.A. Tryk, A. Fujishima, S.M. Park, Chem. Commun. (2002) 486–487.